INTERNATIONAL JOURNAL OF Electroactive Materials

Int. J. Electroactive Mater. 3 (2015) 1–5
www.electroactmater.com

Short Communication

Nanoporous TiO_2 and ZnO Photoelectrodes: A Comparative Photovoltaic Performance Study

Nitin A. Jadhav[1,2,#], S. K. Tomar[3,^], Pramod K. Singh[1,4,"], B. Bhattacharya[1,*]

[1]Materials Research Laboratory, School of Basic Science and Research, Sharda University Greater Noida, 201310, India.
[2]Postgraduate Department of Chemistry Tuljaram Chaturchand College Baramati, Dist Pune Maharashtra, India.
[3]Department of Chemistry Institute of Engineering and Technology, JK Lakshmipat University, Jaipur, 302026, India.
[4]Institute for Microsystems Technology, Vestfold University College, Tonsberg, 3103, Norway.
E-mails Addresses: nitinchem1@gmail.com[#]; sandeeptomar@jklu.edu.in[^]; singhpk71@gmail.com["];
b.bhattacharya@sharda.ac.in*

Received: 6 December 2014 / Accepted: 7 January 2015 / Published: 15 January 2015

ABSTRACT: In present study highly ordered nanoporous TiO_2 materials with crystalline frameworks were successfully synthesized from different concentration of triblock co-polymer (soft templates) like F-127 F-68. Synthesized mesoporous TiO_2 have variation of pore size ranging from 2-5 nm and having high specific surface area from 216 m^2/g - 352 m^2/g. By using same synthesis method Mesoporous ZnO materials also synthesized and we have obtained record highest specific surface area up to 578 m^2/g and average pore size ranging from 7.22 nm to 13.43 nm A photoelectrode fabricated using synthesized mesoporous TiO_2 and ZnO shows increase in photocurrent (J_{sc}) with increase in pore size as well as change in V_{oc} with surface area and particle size with variation in structure texture and morphology of photoelectrode. The DSSC was fabricated using N3 dye as sensitizer and solid polymer electrolyte with KI/I_2 as redox electrolyte. Synthesized samples were characterized by XRD, TEM, and Brunauer-Emmett-Teller (BET). Photovoltaic parameters suggests that dye sensitized solar cell (DSSC) performance is strongly dependent on combined effect of V_{oc} and J_{sc} which shows the characteristic change with structure texture morphology as well as pore size and specific surface area of fabricated electrode.

Keywords: DSSC; TiO_2; Zinc Oxide; Mesoporous; Soft Template

1. Introduction

Wide band gap semiconductors play a key role in many applications such as photovoltaic [1], Catalysis [2,4], sensors [5-8] and drug delivery [9,10]. Till date variety of nanomaterials have been developed and studied in different fields. The field of nanotechnology emerged when material scientist and research have observed that lot of applications are surface phenomenon and as surface area increases the efficiency to the application increases and hence boom of nanotechnology emerged. Recently it is found that the porous materials basically mesoporous materials have vast amount of specific surface area than nanomaterials. As we are aware that wide band gap porous semiconductors such as TiO_2, ZnO and CdO are most promising candidates for fabrication of working electrode in dye sensitized solar cell (DSSC). Modern research is more focus towards developing and modifying these materials. Scientist have concentrated to modify structure texture and morphology of these materials by synthesizing nanomaterials with nanoparticles [11,12] nanowires (or nanorods), [13,14] nanotubes [15] nanobelts [16] nanosheets, [13,17] and nanotips [18,19] structure by keeping in mind that for the efficient device applications nanomaterials having large specific surface area is the prime need of present scenario. In recent days it is found that nanomaterials with porous morphology is an additional important feature for device application. Very recently nanostructures with highly ordered porous network and having large specific surface area with optimum pore size have been developed i.e. TiO_2 [20-23], ZnO [24,25-26], SiO_2 [27-29] and SnO_2 [30]. Out of these the crystalline TiO_2 is most widely used photoelectrode for fabrication of DSSC but due to its more advanced photocatalytic property some efforts are also found on fabrication of DSSC using ZnO as working electrode. These days DSSC technology based on ZnO photoelectrode has been explored extensively. ZnO is a wide-band-gap semiconductor that possesses an energy-band structure and physical properties similar to those of TiO_2 but has higher electronic mobility that would be favorable for fast electron transport, with reduced recombination loss when used in DSSCs. Many studies have already been reported on the use of ZnO material for application in DSSCs. ZnO is distinguished alternative to TiO_2 due to its ease of crystallization and anisotropic growth. These properties allow ZnO to be produced in a wide variety of nanostructures, thus possessing unique properties for electronics, optics, or photocatalysis. Recent studies on ZnO-nanostructure-based DSSCs have delivered many new concepts, leading to a better understanding of photoelectrochemically based energy conversion [24-26,31]. This, in turn, would speed up the development of DSSCs that are associated with TiO_2. One of the defining features of nanostructures is their size on the nanometer scale. This, first of all, provides the nanostructures with a large specific surface area. It

also result in many particular behaviors in electron transport or light propagation in view of the surface effect.

In the present article we have reported comparative photovoltaic studies of crystalline mesoporous ZnO with mesoporous TiO_2. The importances of surface area with photovoltaic performance are also presented in detail.

2. Experimental Section

Materials: Titanium tetrabutoxide ($Ti(OC_4H_9)_4$, 97.0%, Aldrich), Pluronic F-127 (extra pure, Sigma Aldrich), ethyl alcohol (C_2H_5OH, 94.0%, Samchun Chemicals), HCl (35.0-37.0%, Samchun Chemicals), Zinc acetate (Fisher Scientific), Methyl alcohol (CH_2OH, Rankem Chemicals) and Sodium Hydroxide NaOH (Fisher Scientific) were used as received without further purification.

Synthesis: The synthesis of mesoporous TiO_2 were carried through triblock copolymer-templated sol-gel method via an evaporation-induced self-assembly (EISA) process. For preparing Ti-sol, 2.7 ml (0.38M) of titanium tetrabutoxide was dissolved and stabilized in 2.9 ml of 35% HCl solution, under vigorous magnetic stirring for 3 h. Ethanol solution of Pluronic F-127 were prepared by adding different amounts of either of the copolymers in 15.2 ml of ethanol (94%) under vigorous magnetic stirring for 3 h. The amounts of the Pluronics were varied to vary their concentrations in the final mixture solution as 0.001 M, 0.0025 M, 0.005 M, and 0.01 M. The previously prepared yellowish Ti-sol was then added to the Pluronic solutions dropwise under magnetic stirring. The stirring process was continued for 12 h until the mixture become colorless and transparent. The resulting mixtures were then aged to form white colored gel. The same procedure have been followed for synthesis of mesoporous ZnO here concentration of F-127 have been kept constant and NaOH concentration was varied as 0.15 M, 0.2 M, 0.25 M, 0.3 M, 0.35 M, 0.4 M, 0.45 M, 0.5 M to study the effect of base concentration on neucleation and growth of ZnO.

Fabrication of DSSC: The resulting paste was then used to fabricate working electrode by doctor blade method on cleaned and blocking layer coated FTO glass and calcinated at 315 °C for 12 h at heating rate of 1 °C/ minute. Calcinated working electrode then soaked in (0.5 mM ethanol) dye solution for overnight and washed with ethanol to remove excess of dye adsorbed on surface of electrode. Solid polymer electrolyte was prepared by desolving PEO:PEG blend in acetonitrile and adding NaI and I_2 with w/w % as 75:25 and 10 w/w % of iodine with NaI dissolved in acetonitrile with 24 h stirring. Also platinum counter electrode was prepared by spin coating of H_2PtCl_6 solution on clean FTO Glass a drop of above prepared electrolyte was sandwiched between fabricated working electrode and counter electrode.

Characterizations: The structure texture and morphology of synthesized samples were examined using JEOL, JEM-2010 and JEOL JEM 2100F transmission electron microscopes operating at 200 kV. For the TEM analysis small amount of sample was dispersed into 95% ethanol. For the structural determination, powder X-ray diffraction patterns were recorded with Rigaku X-ray diffractometer using the CuKα radiation (λ = 1.5405 Å). Surface area, pore volume, pore size distribution and pore diameter were measured by BET Quantachrome Autosorb AS1win instrument. To analyze pore size sample is outgased at 300 °C for 7 h. The *Voc Jsc* FF and photo current conversion efficiency was measured by Keithley source meter model no. 4200.

3. Results and Discussion

From Nitrogen adsorption/desorption isotherms of mesoporous TiO_2 and Mesoporous ZnO samples were analyzed using BET instrument and shown in **Figure 1**. It is noticed, that all the samples revealed similar and type-IV isotherms (IUPAC classification) which is associated to mesopores of high degree of pore size uniformity with a sharp desorption at about P/P_0 = 0.45, indicating sudden evaporation of adsorbate from cylindrical shaped pores. And from which specific surface area and average pore size can be calculated.

Figure 2 shows the variation of specific surface area versus the mesoporous TiO_2 and ZnO samples. It is clear from comparative study **(Figures 2a and 2b)** that both the samples shows that as template concentration

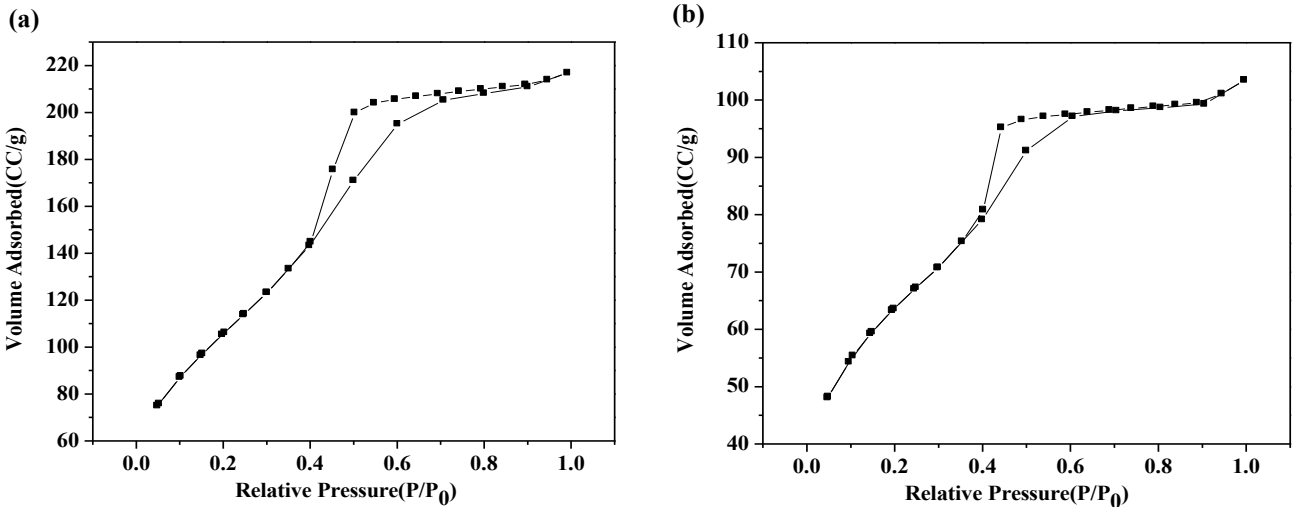

Figure 1: Representative Nitrogen adsorption/desorption isotherms for the mesoporous (a) TiO_2 and (b) ZnO samples synthesized and calcinated at 315 °C for 12 h

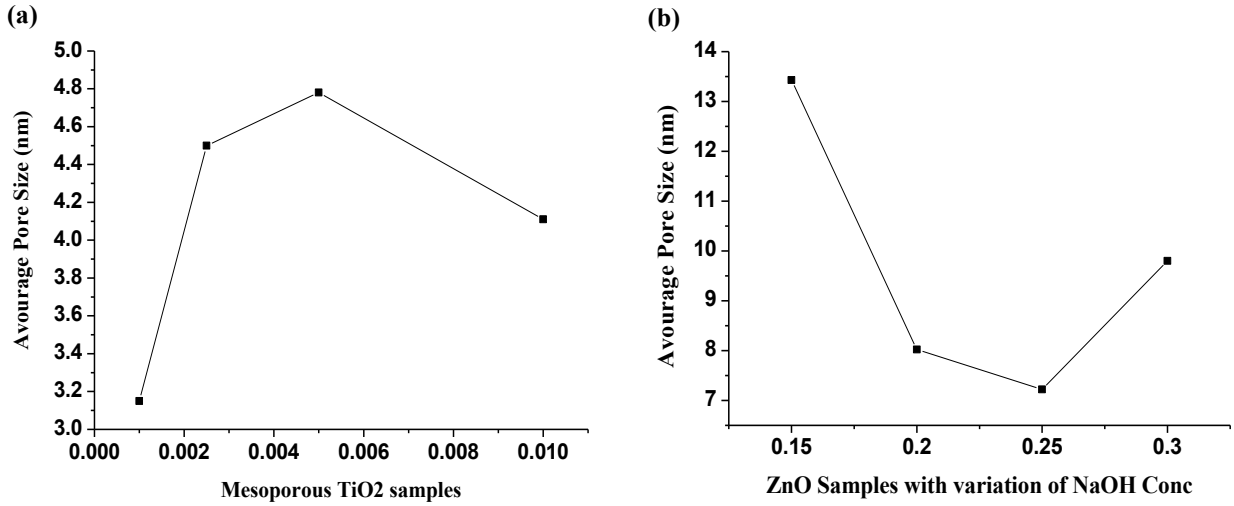

Figure 2: Variation of Specific surface area versus the mesoporous TiO_2 samples (a) and variation of specific surface area versus the mesoporous ZnO samples (b)

(in TiO_2 case) and base concentration increases surface area increases this happens as in case of TiO_2 template concentration increase number of formed pore also increases which leads to increase in surface area. As we know that in case of TiO_2 surfactant Pluronics acts as template to form porous structure. As concentration of template increases, the number of pores presents on surface of TiO_2 increases and as number of pore increases, it leads to increase in specific surface area. In case of ZnO as concentration of NaOH increases which leads to increase hydrolysis rate and it affects nucleation and growth rate hence surface area increases.

Figure 3 shows the variation of Average pore size in the mesoporous TiO_2 and ZnO samples. The average pore size in TiO_2 is optimum for a certain concentration of the Pluronic, and then it decreases **(Figure 3a)**. The decrease of pore size at high copolymer concentration might be due to the steric hindrance occurred when number of micelles is large in solution due to high concentration of Pluronic. In case of mesoporous ZnO, we can see at lower base concentration larger pore size formation takes place but at as concentration, there is sudden decrease in pore size **(Figure 3b)** this happens due to increase in hydrolysis rate and faster nucleation and growth of ZnO takes place.

3.1 Dye Sensitized Solar Cells

The synthesized TiO_2 and ZnO paste were used to fabricate the working electrode of DSSCs. The photo current density-voltage (*J-V*) characteristics of the DSSCs fabricated with the different morphologies of TiO_2 and ZnO photoanodes are shown in **Figure 4** and all the parameters are summarized in **Table 1**.

From **Table 1**, it is observed that the obtained J_{sc} values follows the same trends which is followed by pore size i.e. the cells fabricated using photoelectrode with higher pore size value of J_{sc} is high and at lower pore size value of J_{sc} is low. As pore size increase the J_{sc} value also increases (in case of TiO_2) and as pore size decreases J_{sc} also decreases (in case of ZnO). This fact is due to radius of gyration of polymers used in electrolyte (for PEO radius of gyration is 13.7 nm) as pore size increase than radius of gyration of polymer there are lot of chances of polymer chain to penetrate inside the pores of electrode and side

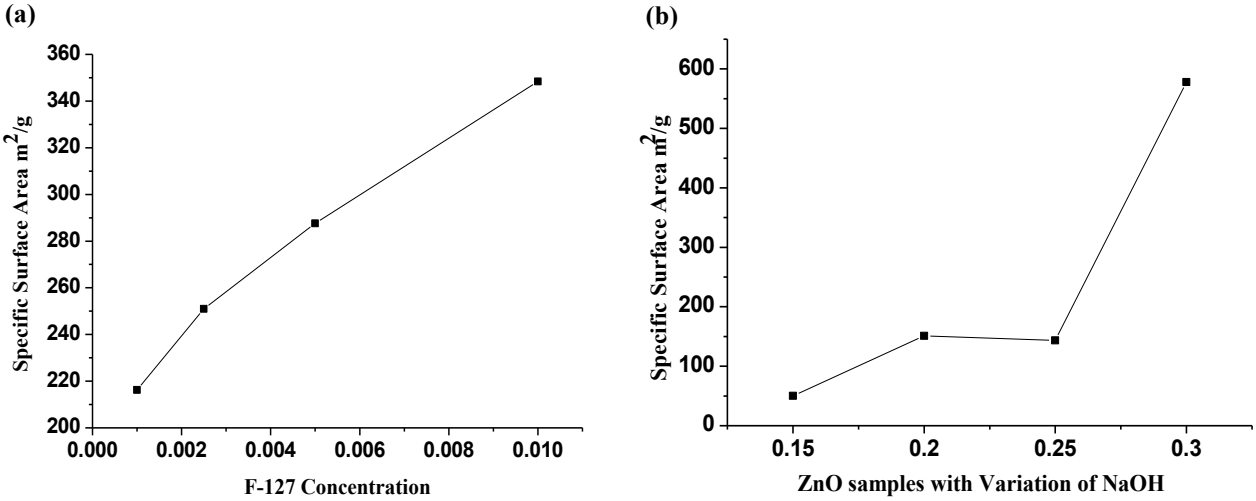

Figure 3: Variation of Average pore size versus the mesoporous TiO_2 samples (a) and variation of average pore size versus the mesoporous ZnO samples (b)

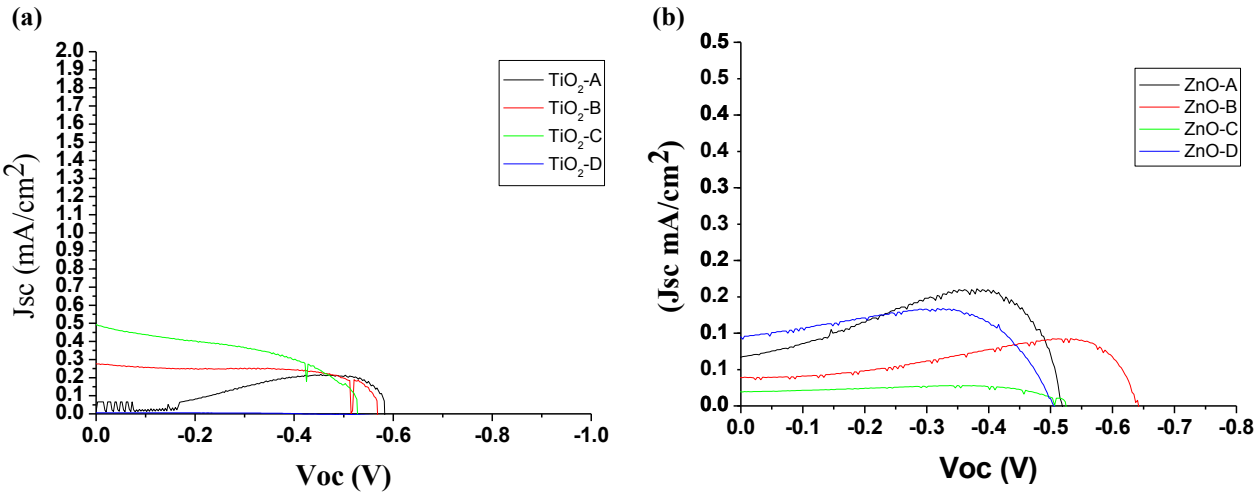

Figure 4: *J-V* curve for mesoporous TiO_2 samples (a) and ZnO samples (b) recorded at 1 sun condition

pores resulting photocurrent may decrease. If we compare TiO_2 photoelectrode with ZnO photoelectrode J_{sc} value for ZnO is much higher than J_{sc} of TiO_2 .The one of the reason behind this is ZnO has higher electronic mobility that would be favorable for fast electron transport, with reduced recombination loss when used in DSSCs and also pore size of synthesized mesoporous ZnO exchange of electrons with dye molecule adsorbed on surface of electrode as well as the dye molecule inside pore get reduced through polymer electrolyte and hence photocurrent get increased, as pore size decreases. It is difficult for polymer chain to penetrate inside pore and make exchange of electrons with dye molecule adsorbed in is much higher (13.43 nm) than synthesized mesoporous TiO_2 (4.78 nm).

Also from **Table 1**, it is observed that in case of mesoporous ZnO, the V_{oc} follows the trend of particle size i.e as particle size increases V_{oc} increase and as particle size decrease V_{oc} decreases. It is well known that V_{oc} is the potential difference between the redox potential of counter electrode and the conduction band of the working electrode. Hence at smaller sizes of the particle, the band structure does not present inside these particles. It is only the compact structure of these particles which is acts as equivalent to the band structure. In such condition, smaller particles will result to incomplete band structure and hence the flat band potential will become lower [31]. Any increase in particle size will lead to better band formation, proper band bending and higher flat band potential. Such change will not only affect on the V_{oc}, but also lead to varied overlapping of the bands of ZnO and excited level of the dye and hence change in photocurrent. But in case of mesoporous TiO_2 as shown in plot the V_{oc} is inversely proportional to specific surface area i.e. as specific surface area increases V_{oc} decreases. The reason behind this is also same as we observed in case of mesoporous ZnO samples, where surface area increases (number of pores present on TiO_2 surface increases) and direct contact of TiO_2 surface to electrolyte decreases as a result extend of formation of interface between electrode-electrolyte decreases and ultimately V_{oc} also decreases. The overall efficiency of DSSC fabricated using TiO_2 and ZnO mesoporous electrodes are calculated and noted in **Table 1**. As we know that the photocurrent conversion efficiency in DSSC is the resultant product of V_{oc} and J_{sc} so overall increase and decrease in conversion efficiency for both samples mesoporous TiO_2 and ZnO are due to increase or decrease in V_{oc} as well as J_{sc}.

Table 1: Surface area, pre size and photovoltaic parameters of TiO_2 and ZnO sample

Samples	Specific Surface area (m^2/g)	Average Pore size (nm)	V_{oc} (V)	J_{sc} (mA/cm^2)	Efficiency (%)
TiO_2-A	216.2	3.15	0.582	2.183×10^{-1}	0.107
TiO_2-B	251	4.5	0.568	2.773×10^{-1}	0.104
TiO_2-C	287.6	4.78	0.528	4.939×10^{-1}	0.122
TiO_2-D	348.4	4.11	0.417	2.306×10^{-1}	0.056
ZnO-A	50.41	13.43	0.4874	1.00	0.2878
ZnO-B	151.1	8.02	0.6223	5.78×10^{-1}	0.3181
ZnO-C	143.5	7.22	0.5103	1.75×10^{-1}	0.1136
ZnO-D	578	9.80	0.5553	8.36×10^{-1}	0.2112

4. Conclusions

We have introduced synthesis strategy for mesoporous TiO2 and mesoporous ZnO powder in bulk amount through triblock copolymer-templated sol-gel method via an evaporation-induced self-assembly (EISA) process. As we know powdered photocatalyst are efficient in its catalytic activity due to its simplicity. In the present article we have modified the working electrode of DSSC. We have modified the structure texture morphology and also pore size as well as surface area. We have successfully synthesized mesoporous TiO_2 and ZnO with highest specific surface area and variation of pore size. Also we have studied the effect of increase or decrease in pore size on short circuit current of DSSC and effect of increase or decrease in particle size as well as specific surface area on open circuit voltage of DSSC. These findings will helps us as well as scientific committee for modifying the other component of DSSC to improve the cell performance.

Acknowledgement

One of the author Mr. Nitin A. Jadhav is very much grateful to Council of Scientific and Industrial Research, Govt. of India for providing financial support for his doctoral research through CSIR-SRF (S/1078(0001)/12 EMR-1. Also we acknowledge DST for funding research project no. DST/TSG/PT/2012/51-C on Dye Sensitized Solar Cells.

References

1. A. Hagfeldt, G. Boschloo, L. Sun, L. Kloo, H. Pettersson, Chem. Rev. 110 (2010) 6595.
2. E. Evgenidou, K. Fytianos, I. Poulios, Appl. Catal. B 59 (2005) 81.
3. M. Saito, T. Fujitani, M. Takeuchi, T. Watanabe, Appl. Phys. A: Mater. Sci. Process. 138 (1996) 311.
4. N.A. Jadhav, P.K. Singh, H.W. Rhee, S.P. Pandey, B. Bhattacharya, Int. J. Electrochem. Sci. 9 (2014) 5377.
5. Z. Fan, J.G. Lu, Appl. Phys. Lett. 86 (2005) 123510.
6. T. Gao, T.H. Wang, Appl. Phys. A: Mater. Sci. Process. 80 (2005) 1451.
7. H.J. Lim, D.Y. Lee, Y.-J. Oh, Sens. Actuators A 125 (2006) 404.
8. L.J. Bie, X.N. Yan, J. Yin, Y.Q. Duan, Z.H. Yuan, Sens. Actuators B 126 (2007) 604.
9. Z.L. Wang, J. Song, Science 312 (2006), 242.
10. Z.L. Wang, J. Phys.: Condens. Mater 16 (2004) R829.
11. E.A. Meulenkamp, J. Phys. Chem. B 102 (1998) 5566.
12. M. Vafaee, M.S. Ghamsari, Mater. Lett. 61 (2007) 3265.
13. S. Kar, A. Dev, S. Chaudhuri, J. Phys. Chem. B 110 (2006) 17848.
14. P.D. Yang, H.Q. Yan, S. Mao, R. Russo, J. Johnson, R. Saykally, N. Morris, J. Pham, R.R. He, H.J. Choi, Adv. Funct. Mater 12 (2002) 323.
15. Q.C. Li, V. Kumar, Y. Li, H.T. Zhang, T.J. Marks, R.P.H. Chang, Chem. Mater: 17 (2005) 1001.
16. X.D. Wang, Y. Ding, C.J. Summers, Z.L. Wang, J. Phys. Chem. B 108 (2004) 8773.
17. M. Fu, J. Zhou, Q.F. Xiao, B. Li, R.L. Zong, W. Chen, J. Zhang, Adv. Mater. 18 (2006) 1001.
18. U. Pal, J.G. Serrano, P. Santiago, G. Xiong, K.B. Ucer, R.T. Williams, Opt. Mater. 29 (2006) 65.
19. G.S. Zhdanov, A.D. Manukhova, M.S. Lozhkin, B. Russ. Acad. Sci. Phys. 78 (2014) 881.
20. N.A. Jadhav, C.W Kim, U. Pal, J. Kim, Y.S. Kang, J. Nanosci. Nanotechno. 12 (2012) 5638.
21. E.L. Crepaldi, G.J.A.A. Soler-Illia, D. Grosso, F. Cagnol, F. Ribot, C. Sanchez, J. Am. Chem. Soc. 123 (2003) 9770.
22. D. Grosso, G.J.A.A. Soler-Illia, E.L. Crepaldi, F. Cagnol, C. Sinturel, A. Bourgeois, A. Brunet-Bruneau, H. Amenitsch, P.A. Albouy, C. Sanchez, Chem. Mater. 15 (2003) 4562.
23. N. A. Jadhav, P.K. Singh, H. W. Rhee, B. Bhattacharya, Nanoscale Res. Lett. 9 (2014) 575.
24. U. Pal, C. W. Kim, N. A Jadhav, Y. S. Kang, J. Phys. Chem. C 113 (2009) 14676.
25. S.Bhattacharyya, A. Gedanken, Micropor. Mesopor. Mat. 110 (2008) 553.
26. S. Bhattacharyya, A. Gedanken, J. Phys. Chem. C 112 (2008) 659.
27. F. Kleitz, D. Liu, G.M. Anilkumar, I.-S. Park, L.A. Solovyov, A.N. Shmakov, R. Ryoo, J. Phys. Chem. B 107 (2003) 14296.
28. Y.S. Kang, H.I. Lee, Y. Zhang, H.Y. Jin, J.E. Yie, G.D. Stucky, J.M. Kim, Chem. Commum (2004), 1524.
29. J. Fan, C. Yu, J. Lei, Q. Zhang, T.Li, B. Tu, W. Zhou, D. Zhao, J. Am. Chem. Soc. 127 (2005) 10794.
30. J. Ba, J. Polleux, M. Antonietti, M .Niederberger, Adv. Mater. 17 (2005) 2509.
31. V.K. Singh, B. Bhattacharya, S. Shukla, P.K. Singh, Materiali in Technologije 49 (2015) 155.